



# Optimizing synthesis strategies for the production of single-phase zirconates with Ce and Nd co-doping

Selina Richter<sup>1</sup> · Sara E. Gilson<sup>1</sup> · Luiza Braga Ferreira dos Santos<sup>1</sup> · Nina Huittinen<sup>1,2</sup>

Received: 19 December 2023 / Accepted: 25 January 2024 / Published online: 8 February 2024  
© The Author(s) 2024

## Abstract

Zirconia-based ceramics are promising host matrices for the immobilization of radionuclides in high-level waste streams due to their high radiation resistance and chemical stability. This study explores coprecipitation and different solid-state synthesis techniques to produce phase-pure zirconia-based ceramics with varying cerium and neodymium co-doping. Varying the dopant concentration enabled the synthesis of zirconates with monoclinic, cubic defect fluorite, and cubic pyrochlore structures. Powder X-ray diffraction was used for phase identification. In the case of coprecipitation, all synthesized compositions were predominantly phase-pure. Solid-state synthesis techniques included manual mixing of metal oxide powders with mortar and pestle, mechanical mixing in a ball mill, and magnetic mixing in a slurry. All solid-state mixing methods produced heterogeneous ceramics, featuring multiple phases, with manual mixing yielding the most phase-pure product. Extending the grinding time, re-sintering of the solid phases, and an increased Nd content were found to enhance the phase purity.

## Introduction

High-level waste (HLW) streams from the reprocessing of nuclear fuel contain transuranium elements like neptunium, americium, and curium, and residual non-separated plutonium. These elements retain their radiotoxicity over extended periods due to their long half-lives (10–10<sup>6</sup> years). To prevent their release into the environment and enable secure storage in deep geological repositories, these elements need to be immobilized within a solid matrix [1]. At present, borosilicate glasses are the most commonly utilized waste forms, primarily due to their flexibility in incorporating a wide variety of elements [1, 2]. Nevertheless, glasses possess certain limitations, such as the limited solubility of actinides within them. Ceramic waste forms offer an alternative to glasses, allowing for increased waste loadings [1].

A crucial criterion for nuclear waste forms is high radiation tolerance, signifying that the structure of the waste matrix should be resistant to damages stemming from

self-irradiation, mainly caused by the  $\alpha$ -decay of the incorporated actinides and associated daughter recoil of the decay products [1]. Moreover, they should exhibit good chemical stability to prevent dissolution and leaching of radionuclides in the event of canister failure within the final repository [1, 3].

Zirconia (ZrO<sub>2</sub>) based ceramics offer promising host matrices for the immobilization of radionuclides found in HLW [4]. Under atmospheric pressure, ZrO<sub>2</sub> is known to exist in three different polymorphs. Monoclinic zirconia ( $P2_1/c$ ) is stable up to 1170 °C, above which a transition to the tetragonal polymorph ( $P4_2/nmc$ ) occurs, followed by a transformation to cubic zirconia ( $Fm\bar{3}m$ ) at temperatures exceeding 2370 °C [5, 6]. Ceramics with cubic crystal structures are preferred nuclear waste forms as they have been shown to be highly radiation resistant [7, 8]. In order to stabilize the high-temperature cubic zirconia phase at ambient temperature, other metal oxides can be added as dopants [9]. The introduction of dopants at defined concentrations can lead to the formation of the cubic pyrochlore phase ( $Fd\bar{3}m$ ). Pyrochlore can be defined by the general formula A<sub>2</sub>B<sub>2</sub>X<sub>6</sub>YZ [10, 11]. The A site is typically occupied by a trivalent rare earth element whereas the B site is preferred by 3d, 4d, and 5d transition metals. Oxygen anions are usually located at the X site [10]. The Y site is typically also filled by an anion such as oxygen, hydroxyl, or fluoride [12]. Z is a vacancy, which is formed as a result of charge compensation [11]. In

✉ Nina Huittinen  
n.huittinen@hzdr.de

<sup>1</sup> Institute of Resource Ecology, Helmholtz-Zentrum Dresden-Rossendorf, Bautzner Landstraße 400, Dresden, Germany

<sup>2</sup> Institute of Chemistry and Biochemistry, Freie Universität Berlin, Fabeckstraße 34-36, Berlin, Germany

a pyrochlore (Fig. 1), the Z sites are ordered and are located around the B cations. In the defect fluorite structure (Fig. 1), the vacancies are disordered and can be situated at any of the X, Y, and Z sites [10].

Similarly to the fluorite-type zirconates, the pyrochlore derivatives also show considerable potential as waste matrices due to their high radiation tolerance. More specifically, certain zirconate pyrochlore compositions have been shown to remain crystalline when subjected to irradiation, and to undergo a phase transition to the cubic defect fluorite crystal structure [13, 14]. In contrast, titanate pyrochlores show a tendency to transform into an X-ray amorphous state, when subjected to heavy-ion irradiation employed to mimic the recoil of daughter nuclei resulting from the  $\alpha$ -decay of actinides [13].

An interesting question that warrants additional studies is the relative radiation tolerance of different zirconate polymorphs. To investigate this, phase-pure ceramics are required. Therefore, in the current study, different synthesis methods for obtaining phase-pure zirconate ceramics co-doped with Ce and Nd at different concentrations were investigated. Hereby, cerium was used as a surrogate for tetravalent actinides such as plutonium due to its similar ionic radius and oxidation state stability.

## Materials and methods

Different compositions of Ce-/Nd-co-doped zirconates were synthesized via coprecipitation and solid-state methods as outlined in Table 1.

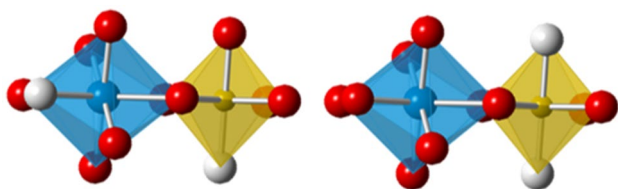


**Fig. 1** Defect fluorite (left) and pyrochlore structure (right). A cations are shown in blue, B cations in yellow, oxygen in red, and vacancies in white

For the coprecipitation route,  $\text{ZrOCl}_2 \cdot 8 \text{H}_2\text{O}$  (Sigma-Aldrich) was dissolved in 0.01 M  $\text{HNO}_3$  (Sigma-Aldrich) to obtain a  $\text{Zr}^{4+}$  solution. Stock solutions of  $\text{Ce}^{3+}$  and  $\text{Nd}^{3+}$  with concentrations of 1.67 M and 1.63 M, respectively, were obtained by dissolving  $\text{CeCl}_3 \cdot 6 \text{H}_2\text{O}$  (Alfa Aesar) and  $\text{Nd}(\text{NO}_3)_3 \cdot 6 \text{H}_2\text{O}$  (Sigma-Aldrich) in MilliQ water. Appropriate amounts of the  $\text{Ce}^{3+}$  and  $\text{Nd}^{3+}$  stock solutions were added to the  $\text{Zr}^{4+}$  solution to achieve the targeted dopant concentrations. A precipitate was produced via the addition of 12.5%  $\text{NH}_4\text{OH}$  (Sigma-Aldrich) according to the reverse dropping method outlined by Chen et al. [15]. The precipitate was aged at room temperature for 6 h, washed six times with MilliQ water to remove ammonia residues, and dried at 60 °C for 24 h. It was thereafter ground with mortar and pestle to produce a homogenous powder before calcination at 600 °C for 2 h in high-purity alumina crucibles. The calcined product was ground again and pressed into pellets of 8 mm diameter by applying a force of 5 kN. The pellets were sintered at 1500 °C for 48 h to obtain ceramics.

The solid-state synthesis route was similar to the coprecipitation synthesis, however, the acidic metal-ion solutions were precipitated separately in 12.5%  $\text{NH}_4\text{OH}$  to yield the respective hydroxides, dried at 60 °C for 24 h, ground, and calcined at 800 °C for 2 h to yield metal oxides. The material was once more ground separately with mortar and pestle to achieve a finely powdered product. After that, three different methods were employed for mixing the metal powders. Manual mixing was done by grinding the powders together with mortar and pestle by hand. The grinding time was varied between 5 and 10 min. Mechanical mixing was conducted in a tungsten carbide ball mill with milling times of either 10 or 20 min. Finally, magnetic mixing was done by adding the respective amount of metal oxide powders to 2 ml Milli Q water to create a slurry. It was stirred with a magnetic stirrer for 2 h followed by drying at 60 °C for 24 h. The mixed metal oxide powders were pelletized (diameter: 8 mm, applied force: 5 kN) and sintered at 1500 °C for 48 h, identical to the coprecipitated phases. After sintering, select samples were ground to a powder, re-pelletized, and re-sintered under the same conditions.

All samples were characterized via Powder X-ray diffraction (PXRD) using a Rigaku Mini-Flex 600

**Table 1** Composition of synthesized zirconates

Samples	Targeted crystal structure	Zr (mol%)	Ce (mol%)	Nd (mol%)
$\text{Zr}_{0.95}\text{Ce}_{0.05}\text{O}_2^*$	Monoclinic	95	5	–
$\text{Zr}_{0.80}\text{Ce}_{0.05}\text{Nd}_{0.15}\text{O}_{1.925}^*$	Defect fluorite	80	5	15
$\text{Zr}_{0.65}\text{Ce}_{0.05}\text{Nd}_{0.30}\text{O}_{1.85}$	Defect fluorite	65	5	30
$\text{Zr}_{0.50}\text{Ce}_{0.05}\text{Nd}_{0.45}\text{O}_{1.775}$	Pyrochlore	50	5	45
$\text{Zr}_{0.45}\text{Ce}_{0.05}\text{Nd}_{0.50}\text{O}_{1.75}^{**}$	Pyrochlore	45	5	50

\*Synthesis only via coprecipitation route

\*\*Synthesis only via solid-state route

diffractometer with Cu-K $\alpha$  radiation (Cu K $\alpha$  = 1.54 Å), variation of 2 $\theta$  from 3° to 90°, a step size of 0.02°, and a spin speed of 2°/min. PXRD patterns were processed using the Rigaku PDXL2 software package and diffraction patterns reported in the International Centre for Diffraction Data (ICDD) database were used to aid in phase identification.

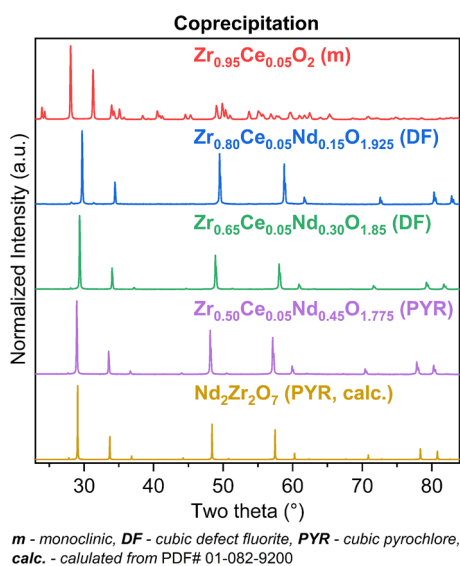
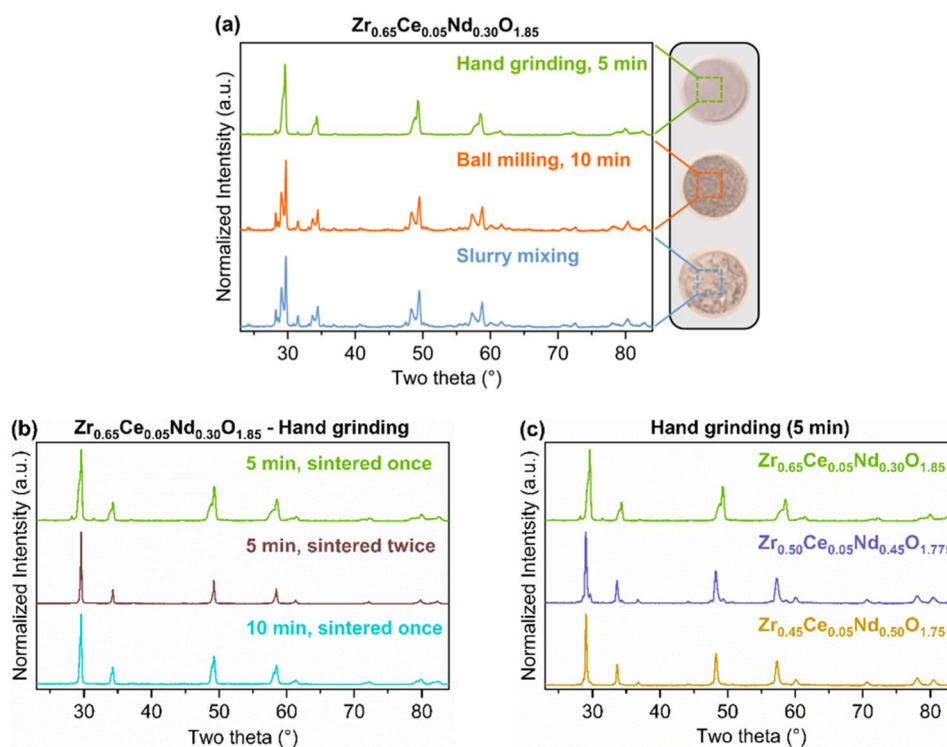


**Fig. 2** XRD-patterns of ceramics obtained by coprecipitation

**Fig. 3** XRD patterns of zirconates obtained through solid-state synthesis. **a** Variation of metal oxide mixing method and the ceramics after sintering. **b** Variation of grinding time and sintering cycles in manually mixed zirconates. **c** Variation of Nd-dopant concentration in manually mixed zirconates



## Results and discussion

As shown in Fig. 2, the ceramics obtained through coprecipitation primarily exhibited a phase-pure monoclinic structure at a low dopant concentration ( $\text{Zr}_{0.95}\text{Ce}_{0.05}\text{O}_2$ ). The addition of the trivalent neodymium cation as a co-dopant resulted in the formation of a cubic defect fluorite phase for the compositions  $\text{Zr}_{0.80}\text{Ce}_{0.05}\text{Nd}_{0.15}\text{O}_{1.925}$  and  $\text{Zr}_{0.65}\text{Ce}_{0.05}\text{Nd}_{0.30}\text{O}_{1.85}$  [16], while the cubic pyrochlore phase was stabilized when increasing the Nd-concentration to 45 mol% ( $\text{Zr}_{0.50}\text{Ce}_{0.05}\text{Nd}_{0.45}\text{O}_{1.775}$ ). The presence of a pyrochlore phase was confirmed by comparing the experimental XRD pattern with a pattern of  $\text{Nd}_2\text{Zr}_2\text{O}_7$  pyrochlore reported in the ICDD database (PDF# 01-082-9200). Other studies have also found the co-precipitation method to yield phase-pure zirconate ceramics under similar conditions [17, 18]. Finkeldei et al. obtained phase-pure defect fluorite and pyrochlores structures in Nd-doped zirconia at a sintering temperature of 1450 °C [19].

After sintering, the ceramics synthesized through solid-state methods, only the manually mixed ones appeared homogenous upon visual inspection as shown in Fig. 3a. The ceramics obtained via mechanical and magnetic mixing seemed to consist of various grains with different colors, indicating the formation of several phases. These could be confirmed by XRD measurements, which generally showed broader and more numerous peaks in the patterns of these ceramics compared to the ceramics obtained through

coprecipitation (Fig. 3a). The ceramics yielded by mechanical and magnetic mixing showed more impurities than the ceramics produced by manual mixing. Through comparison of the positions of the additional peaks with XRD patterns reported in the ICDD database, the main impurity phases could be identified as  $ZrO_2$ ,  $CeO_2$ , and  $Nd_2O_3$  along other zirconate phases with varied compositions. This suggests inadequate mixing of the metal oxide powders during the synthesis process. Increasing the milling time from 10 to 20 min during mechanical mixing did not improve the phase-purity of the resulting ceramic. This is in agreement with results published by Jarlingo et al. who used wet ball milling of  $La_2O_3$  and  $ZrO_2$  in ethanol followed by 1 h of sintering at 1500 °C to obtain  $La_2Zr_2O_7$ . After one hour of milling, XRD measurements showed  $La_2Zr_2O_7$  to be present alongside residual  $La_2O_3$  and  $ZrO_2$ . By increasing the milling time to 9 h, they were able to obtain single-phase  $La_2Zr_2O_7$ . [20] In Jiang et al. [21], the synthesis of single-phase  $Fe^{3+}$  stabilized cubic zirconia through the sole use of high-energy ball milling without subsequent sintering was reported. However, such mechanochemical syntheses require significantly longer milling times of up to 110 h. [21]

The XRD patterns of the ceramics synthesized with manual mixing exhibited broadened peaks at the same positions as those in the coprecipitated ceramics, with almost no additional peaks. This implies that the desired cubic defect fluorite and cubic pyrochlore phases were stabilized. Therefore, manual mixing can be considered the best one out of the three mixing methods. A study by Laverov et al. demonstrated the feasibility of producing Gd-doped zirconate pyrochlores by solid-state synthesis via hand grinding and sintering at 1500–1550 °C for up to 40 h. However, the samples were not completely homogeneous, as compositional variations were detected in different areas of the sample [22]. Based on these outcomes, optimization attempts were undertaken to achieve ceramics with improved phase-purity. One of the strategies used involved re-sintering of the ceramics, as it has been shown by Hellwig et al. that re-sintering and extended sintering times could facilitate complete phase transformation, resulting in an improvement of phase purity of yttria stabilized zirconia containing Er and Pu [23]. Following re-sintering, the hand-ground Ce/Nd-co-doped zirconate ceramics showed a significant narrowing of the diffraction peaks signifying enhanced order and phase purity (Fig. 3b). This also stands in agreement with a study by Harvey et al. who obtained phase-pure ceramics with composition  $(La_{1-x}Nd_x)_2Zr_2O_7$  in cubic and monoclinic phases after re-sintering [24]. In order to elucidate the role of additional grinding during the re-sintering process in the improved phase purity, another ceramic where the metal oxide powders were ground together for 10 min instead of 5 min was produced and analyzed. The XRD pattern displayed narrower peaks compared to the ceramic

where the educts were ground for 5 min. However, this difference is less pronounced than in the case of re-sintering. Consequently, it can be asserted that although an extension of grinding time contributes to achieving enhanced phase purity, re-sintering the ceramics results in a more substantial improvement of phase purity. Finally, when comparing the ceramics where the metal oxide powders were ground for 5 min, samples with the highest Nd content exhibited narrower peaks in their XRD patterns. This is demonstrated in Fig. 3c for the pyrochlore compositions with differing Nd concentrations.

## Conclusions

In the present study, various compositions of phase-pure Ce/Nd-co-doped zirconate ceramics were successfully synthesized by coprecipitation. The type of crystal phase formed was contingent of the dopant concentration. With the excellent homogeneity of monoclinic and cubic zirconates containing different trivalent- and tetravalent dopant loadings, direct coprecipitation routes of aqueous actinide-bearing waste streams with zirconium solutions show great potential for the generation of single-phase ceramic waste forms. By applying solid-state synthesis methods, manual mixing of the metal oxide powders with mortar and pestle proved to be the most effective mixing technique considering the applied mixing times. A long grinding time as well as re-sintering of the ceramics improved the phase-purity. Proper mixing and grinding of the educts alongside adequate sintering temperatures and sintering times are prerequisites when producing ceramics via solid-state routes. The results show that, for solid actinide-bearing wastes, such as separated stock piles of U,Pu oxides, powder metallurgical methods can be used. Single-phase ceramics will, however, require long powder milling times for the generation of single-phase ceramics, which can increase the risk of contamination with radioactive dust.

Finally, with the achieved phase-pure cubic Ce/Nd-co-doped zirconate phases, their relative radiation tolerance, which is one of the prerequisites for their use as waste matrices, can be explored in a next step using external heavy ion irradiation.

**Author contributions** SR: formal analysis and investigation, writing—original draft preparation, writing—review and editing, SG: conceptualization, methodology, writing—review and editing, supervision, LBFS: methodology, writing—review and editing, NH: conceptualization, methodology, writing—review and editing, funding acquisition, supervision.

**Funding** Open Access funding enabled and organized by Projekt DEAL. This work was supported by the German Federal Ministry of

Education and Research (BMBF) under the AcE project (02NUK060). Bundesministerium für Bildung und Forschung, 02NUK060, Nina Huitinen.

**Data availability** The data that support the findings of this study are available from the corresponding author upon reasonable request.

## Declarations

**Conflict of interest** All authors declare that there is no conflict of interest.

**Consent to publish** All authors consent to the submission of this article.

**Open Access** This article is licensed under a Creative Commons Attribution 4.0 International License, which permits use, sharing, adaptation, distribution and reproduction in any medium or format, as long as you give appropriate credit to the original author(s) and the source, provide a link to the Creative Commons licence, and indicate if changes were made. The images or other third party material in this article are included in the article's Creative Commons licence, unless indicated otherwise in a credit line to the material. If material is not included in the article's Creative Commons licence and your intended use is not permitted by statutory regulation or exceeds the permitted use, you will need to obtain permission directly from the copyright holder. To view a copy of this licence, visit <http://creativecommons.org/licenses/by/4.0/>.

## References

1. W.J. Weber, A. Navrotsky, S. Stefanovsky, E.R. Vance, E. Vernaz, *MRS Bull.* (2009). <https://doi.org/10.1557/mrs2009.12>
2. C.M. Jantzen, in *Handbook of Advanced Radioactive Waste Conditioning Technologies*, ed. By M.I. Ojovan (Woodhead Publishing, 2011), pp. 159
3. N.C. Hyatt, M.I. Ojovan, *Mater.* (2019). <https://doi.org/10.3390/ma12213611>
4. G.R. Lumpkin, *Elements* (2006). <https://doi.org/10.2113/gselements.2.6.365>
5. S. Block, J.A.H. Da Jornada, G.J. Piermarini, *J. Am. Chem. Soc.* (1985). <https://doi.org/10.1111/j.1151-2916.1985.tb15817.x>
6. E.H. Kisi, C.J. Howard, *Key Eng. Mater.* (1998). <https://doi.org/10.4028/www.scientific.net/KEM.153-154.1>
7. P. Kalita, S. Ghosh, G. Gutierrez, P. Rajput, V. Grover, G. Sattonnay, D.K. Avasthi, *Sci. Rep.* (2021). <https://doi.org/10.1038/s41598-021-90214-6>
8. J.-M. Costantini, F. Beuneu, W.J. Weber, *J. Nucl. Mater.* (2013). <https://doi.org/10.1016/j.jnucmat.2013.02.041>
9. S.-M. Ho, *Mater. Sci. Eng.* (1982). [https://doi.org/10.1016/0025-5416\(82\)90026-X](https://doi.org/10.1016/0025-5416(82)90026-X)
10. S. Finkeldei, P. Kegler, P.M. Kowalski, C. Schreinemachers, F. Brandt, A.A. Bukaemskiy, V.L. Vinograd, G. Beridze, A. Shelyug, A. Navrotsky, D. Bosbach, *Acta Mater.* (2017). <https://doi.org/10.1016/j.actamat.2016.11.059>
11. S. Finkeldei, M.C. Stennett, P.M. Kowalski, Y. Ji, E. de Visser-Týnová, N.C. Hyatt, D. Bosbach, F. Brandt, *J. Mater. Chem. A* (2020). <https://doi.org/10.1039/C9TA05795A>
12. D. Atencio, *Front. Chem.* (2021). <https://doi.org/10.3389/fchem.2021.713368>
13. B.D. Begg, N.J. Hess, D.E. McCready, S. Thevuthasan, W.J. Weber, *J. Nuc. Mater.* (2001). [https://doi.org/10.1016/S0022-3115\(00\)00696-6](https://doi.org/10.1016/S0022-3115(00)00696-6)
14. M. Lang, F. Zhang, J. Zhang, J. Wang, J. Lian, W.J. Weber, B. Schuster, C. Trautmann, R. Neumann, R.C. Ewing, *Nucl. Instrum. Methods Phys. Res. B* (2010). <https://doi.org/10.1016/j.nimb.2010.05.016>
15. H. Chen, Y. Gao, Y. Liu, H. Luo, *J. Alloys Compd.* (2009). <https://doi.org/10.1016/j.jallcom.2009.02.081>
16. P. Li, I.-W. Chen, J.E. Penner-Hahn, *J. Am. Ceram. Soc.* (1994). <https://doi.org/10.1111/j.1151-2916.1994.tb05404.x>
17. V. Svitlyk, S. Weiss, C. Hennig, *J. Am. Ceram. Soc.* (2022). <https://doi.org/10.1111/jace.18735>
18. V.M. Bekale, C. Legros, C. Haut, G. Sattonnay, A.M. Huntz, *Solid State Ion.* (2006). <https://doi.org/10.1016/j.ssi.2006.10.004>
19. S. Finkeldei, F. Brandt, A. Bukaemskiy, S. Neumeier, G. Modolo, D. Bosbach, *Prog. Nucl. Energy* (2014). <https://doi.org/10.1016/j.pnucene.2013.07.020>
20. M. Jarlingo, Y.-S. Kang, A. Kawasaki, *Mater. Trans.* (2005). <https://doi.org/10.2320/matertrans.46.189>
21. J.Z. Jiang, F.W. Poulsen, S. Mørup, *J. Mater. Res.* (1999). <https://doi.org/10.1557/JMR.1999.0183>
22. N.P. Laverov, S. Yudintsev, S. Stefanovsky, Y.N. Jang, I.K. Bae, S. Chae, *Dokl. Earth Sci.* **383**, 190 (2002)
23. C. Hellwig, M. Pouchon, R. Restani, F. Ingold, G. Bart, *J. Nuc. Mater.* (2005). <https://doi.org/10.1016/j.jnucmat.2004.11.004>
24. E.J. Harvey, K.R. Whittle, G.R. Lumpkin, R.I. Smith, S.A.T. Redfern, *J. Solid State Chem.* (2005). <https://doi.org/10.1016/j.jssc.2004.12.030>

**Publisher's Note** Springer Nature remains neutral with regard to jurisdictional claims in published maps and institutional affiliations.